Egypt. J. Chem. Vol. 67, SI: M. R. Mahran, pp. **1621 - 1629** (2024)

Egyptian Journal of Chemistry

http://ejchem.journals.ekb.eg/

Investigation of the biological activity of silver nanoparticles biosynthesized from *Echinops ritro L*

Amel Fedol[1,2*], Naima Berbaoui[3]; Habiba Berbaoui[4], Chemseddine D.Khorsi[1] and Bochera Bennaoum[1]

[1]*Département of pharmacy, faculty of medecine, Ahmed Ben Bella University, Oran1. Algeria.*
[2]*Phytochemistry & Organic Synthesis Laboratory,Tahri Mohamed University .Bechar .Algeria*
[3] *Faculty of natural sciences and life, Tahri Mohamed University, Bechar.Algeria*
[4] *Laboratory of Energetic in Arid Zones, solar fields team and its applications, Faculty of Exact Sciences, department of matter sciences, university of Tahri Mohammed Bechar. Algeria*

Abstract

The biosynthesis of silver nanoparticles (AgNPs) is the subject of this investigation using the ethanolic extract of *Echinops ritro L.*, a medicinal plant from the Asteraceae family, and evaluates their antimicrobial properties. A combination of spectroscopic methods was used to characterise the biosynthesised AgNPs. The UV-visible spectrum showed a characteristic absorption band at 415 nm, confirming AgNPs formation investigation revealed several functional groups that contribute to the stabilisation and reduction of AgNPs. XRD confirmed the crystalline nature of the nanoparticles with an average size of 23.36 nm. The antimicrobial activity of the synthesized AgNPs was assessed against five bacterial strains (*Escherichia coli, Enterococcus faecalis, Proteus mirabilis, Enterococcus hirae, and Bacillus cereus*) and one fungal species (*Candida albicans*) using the disc diffusion method. The AgNPs exhibited significant antibacterial activity, with inhibition zones ranging from 5 to 33 mm, depending on the concentration and bacterial strain tested. The *E. coli* bacteria showed the strongest antibacterial activity, with an inhibitory zone measuring 33±12.5 mm at a concentration of 100 µg/mL. The AgNPs also demonstrated antifungal activity against *C. albicans*, with a maximum inhibition zone of 21± mm at 100 µg/mL. This research highlights the potential of *Echinops ritro L*. extract for the green synthesis of AgNPs with promising antimicrobial properties, offering a sustainable approach for developing new antimicrobial agents.

Key words :*Echinops ritro*L,silver nanoparticles ,antimicrobial ,biosynthesis ;

1.Introduction

We interact instantaneously and continuously with the microscopic world of viruses, bacteria, parasites, and other organisms. We have become aware of this fact because of the recent virus outbreak. The microbes that comprise our microbiotas reside within us [1]. Both human and animal bodies are covered in a vast array of bacteria that do not pose a threat to health, including those found on the skin, in the mouth, respiratory system, digestive tract, reproductive system. These microorganisms are referred to as resident blooms or resident microbiomes. The microbial population in our bodies is of comparable magnitude to the number of human cells [2]. Humans can benefit from several native flowers, including those that help regulate diet or stop the spread of more harmful germs [3, 4]. Only a few types of bacteria have the potential to cause illnesses. In rare situations, local bacteria may operate as pathogenic agents and induce illnesses by the production of toxins, tissue invasion, or both. Inflammation caused by specific germs can affect the heart, lungs, neurological system, kidney, or digestive tract. Specific forms of bacteria, including H. pylori, can raise the risk of cancer [5]. After coronary heart disease, Bacterial infections rank as the second leading cause of mortality worldwide [6]. Pneumococcus and Staphylococcus aureus are the two most lethal bacteria. The increasing body of research on biofilm-associated illnesses and multiresistant bacteria calls for developing further bactericidal strategies [7]. The advancement of nanobiotechnologies, particularly the ability to manufacture nanomaterials based on certain metal oxides in size and shape, may contribute to new antibacterial and antifungal agents. It is the sizes of nanoparticles that mostly determine their functional

*Corresponding author e-mail: amelfedol@yahoo.fr.;
Receive Date: 23 August 2024, Revise Date: 16 October 2024, Accept Date: 19 November 2024
DOI: 10.21608/ejchem.2024.313889.10249

activities [8–11]. Except from the chemical and thermal stability of inorganic materials, the occurrence of interesting phenomena like quantum confinement effects, a notable increase in the surface-volume ratio, and a change in the surface energy when metal oxides are reduced to the nanoscale makes their use at the nanoscale very significant. [11–14]. Given that nanoparticles' principal mode of action is direct interaction with the bacterial cell wall, most resistance mechanisms observed with antibiotics, for example, are irrelevant until they need to penetrate the cell wall. It means that nanoparticles (NPs) may be less susceptible to prompting resistance in bacteria compared to antibiotics [7–15]. Silver has been known since ancient times for its therapeutic uses. Until the 1940s, when the first modern antibiotics were discovered and developed and proved to be noticeably more efficient, silver was commonly employed in medicine to treat bacterial infections in the late 19th and early 20th centuries. There are now three ways that silver affects microorganisms that are understood. First, Silver cations can induce cavities and penetrate the bacterial cell wall by their interaction with the peptidoglycan component. [16]. Second, silver ions can penetrate bacterial cells, disrupting metabolic pathways and inhibiting cellular respiration, which produces reactive oxygen species [17]. Finally, silver can disrupt DNA replication [18]. Silver is re-emerging as a viable treatment option in the form of nanoparticles. Silver nanoparticles are produced by a variety of organisms, including higher plants, lichens, bacteria, and fungi. Various plants are used as "factories" to make silver nanoparticles, including medicinal botanicals [19]. Research findings indicate that by combining mineral salts with plant extracts, silver ions establish chemical interactions with proteins and water-soluble compounds by binding to -OH and -COOH substituents. Conformational changes in the protein molecule are induced, which in turn facilitate the conversion of the trapped metal ion into silver [20-21]. Furthermore, the cysteine residues and amino groups of proteins contribute to the reduction of silver and the formation of AgNPs. [22-23]. Alkanes, amines, phenols, polyphenols, arabinose, galactose, aldehydes, ketones, alcohols, alkaloids, lignans, terpenoids, and flavonoids can all serve as "capping" agents in the creation of silver nanoparticles [24-30].The objective of this work is to assess the antibacterial and antifungal characteristics of AgNPs, biosynthetized from an ethanolic extract of the foliage of *Echinops ritro L.*, a medicinal plant Belonging to the Asteraceae family. Echinops plants have been reported to contain a chemical belonging to several classes, such as alkaloids, flavonoids, terpenoids, lipids, steroids, and polyacetylenes [31]. *Echinops ritro* L has been used traditionally to treat inflammation and pain, respiratory and infectious illnesses, skin issues, kidney stones, facial paralysis, and neuritis. In traditional medicine, this plant is utilized for its abortifacient qualities that expedite the ejection of the placenta [32].

2.Materials and methods

2.1. Plant material

In February 2023, *Echinops ritro* L was collected from the Oued Rhio area in Relizane Province, western Algeria. The obtained plant material was dried in the shade. The dried plant mass was crushed and stored in dark, airtight containers until needed.

2.2. Biosynthesis of Silver Nanoparticle

- The biosynthesis of AgNPs was carried out using *Echinops ritro* L materiel plant. About 10g of plant material were suspended in 100 mL of 70° ethanol. To ensure the maximum extraction of bioactive compounds from the plant material, the mixture was subjected to a reflux extraction process lasting 45 minutes at a temperature of 80°C. After the extraction, any solid residues in the liquid were removed through filtration, and the resulting transparent liquid, referred to as solution 1, was transferred to a separate flask for future purposes.

In parallel, a mass of 1.7 grams of silver nitrate (AgNO3) was added to a 100 ml volumetric flask and distilled water was added to completely dissolve the silver nitrate with continuous stirring (solution 2). The ethanolic extract (solution 1) was slowly combined with the silver nitrate solution (solution 2) using a burette to ensure precise measurement. To ensure even distribution and interaction between the components, the final mixture was vigorously stirred. The completed mixture was spun in a centrifuge for 30 minutes at 4000 revolutions per minute (rpm) to clean the silver nanoparticles, and the remaining substance was cautiously gathered and dehydrated in an oven at 70°C for 12 hours. This approach guaranteed the effective production and retrieval of AgNPs from the plant extract.

2.3. Silver nanoparticles characterization

2.3.1. UV-visible spectroscopy

The formation of AgNPs was analyzed using surface plasmon resonance band spectroscopy with UV-Visible spectrophotometry. Spectrophotometric measurements were performed using a double-beam UV-Visible spectrophotometer (Thermo UV-1601)

within the 200–800 nm range, with a 10 nm resolution. Baseline correction was conducted using a blank reference. The reduction of Ag^+ ions in the solution was monitored by periodically sampling the aqueous component and measuring its UV-Vis spectra. The spectrophotometer chamber was maintained at a constant temperature of 25°C.

2.3.2. Fourier transform infrared spectroscopy (FTIR) analysis

Functional groups potentially involved in the synthesis and stabilization of AgNPs were identified using FTIR spectroscopy. The FTIR spectrum was obtained in the 400–4000 cm^{-1} range with a Bruker alpha (Thermo Scientific, Waltham, MA).

2.3.3.X-Ray Diffraction (XRD) Characterization

It is the most widely employed method for analyzing chemical compounds and assessing the crystal structure and size of AgNPs using Cu-Kα radiation with a wavelength of 1.5406 Å. The structure of the synthesized nanoparticles was investigated through X-ray diffraction (XRD).

The AgNPs were ascertained by X-ray diffraction (XRD) using a Shimadzu-XRD 6000 diffractometer, featuring Bragg Brentano geometry and a CuKα source (40 kV, 30 mA) at an incidence angle of 2°. The mean crystallite sizes were calculated using the Debey Scherrer equation.: $D = 0.94\lambda/\beta \cos \theta$. Here, D represents the average crystallite domain size perpendicular to the reflecting planes, λ is the X-ray wavelength, β is the full width at half maximum (FWHM) of the peak, and θ is the diffraction angle.

2.4. Assessment of biological activity

2.4.1. Antibacterial activity

The antibacterial action was studied using five different types of bacteria of *Escherichia coli* (ATCC 8739), *Enterococcus faecalis* (ATCC 45452), *Proteus mirabilis* (ATCC 783CI), *Enterococcus hirae* (ATCC 10541), *Bacillus cereus* (ATCC 10870) bacterial species were provided by undergraduate biology laboratory of Tahri Mohamed, Bechar University. The microorganisms studied are clinically important ones causing several infections, food-borne diseases, spoilages, skin infection and it is essential to overcome them through some active therapeutic agents.

To investigate the antibacterial characteristics of silver nanoparticles, a dispersed system must be created. The nanoparticles are first dispersed in a suitable solvent and then exposed to ultrasonic waves under regulated conditions. A series of DMSO (Dimethyl sulfoxide) dilutions of the synthesized compounds were made. Five solutions were created by diluting masses of (2.5 mg, 5 mg, 10 mg, 50 mg, and 100 mg) into 10 mL of DMSO. The solutions underwent ultrasonic treatment for 30 minutes.

The inoculum was created from a young culture aged 18 to 24 hours on non-selective nutrient agar plates and then incubated at 37°C for 24 hours to maximize growth.

The agar-disc diffusion method was employed to evaluate the antibacterial effectiveness of AgNPs. Bacterial suspensions at a 0.5 McFarland standard were prepared, and a sterile cotton swab was used to create a uniform bacterial lawn on freshly prepared Muller-Hinton agar plates. Five-millimeters discs made from Whatman filter paper were sterilized, and 10 µL of different concentrations (2.5µg/mL,5 µg/ml, 10 µg/mL, 50µg/mL, and 100 µg/mL) of AgNPs were applied to the sterile discs under aseptic conditions before placing them on the agar surface. **H**émi-synthétique **L**incosamide **S**pécifque(clindamycin) served as the positive control, while DMSO was used as the negative control. After incubating the plates for 24 hours at 37°C, the effectiveness of AgNPs was assessed by measuring the inhibition zones in millimeters. Each experiment was conducted three times, and the average inhibition zones were recorded for all trials [33].

2.4.2. Antifungal activity

Candida albicans fungi were obtained from the Department of Biology, Ahmed Ben Bella University. The antifungal effectiveness of AgNPs against *Candida albicans* was assessed using a disc diffusion assay. Fungal strain was spread on Sabouraud dextrose agar to create a uniform lawn using the spread plate technique. Sterile filter discs containing various concentrations (2.5µg/mL, 5 µg/mL, 10 µg/mL, 50µg/mL, and 100 µg/mL) of AgNPs were placed on the agar surface under sterile conditions. The plates were then incubated 18 hours at 35°C. After incubation, the zones of inhibition around each disc were measured in millimetres. Amphotericin B served as a positive control, while DMSO was used as a negative control. All tests were conducted in triplicate, and average inhibition zones were calculated for each trial [34].

2.5. Statistical analysis

Statistical analysis was performed with IBM SPSS statistics 25.0. Data were expressed as means ± standard deviation (SD). Comparisons between groups were performed with analysis of non-parametric test. A value of $P < 0.05$ was considered statistically significant (table 1).

3.Results and discussion

3.1. Characterization of silver nanoparticles

3.1.1. UV-Visible spectrophotometer analysis

The first indication of the formation of AgNPs is the visual color change in the reaction mixture [35]. Nanoparticle formation started when the extract was combined with the silver nitrate solution. The visible colour of the solution shifted from bright yellow to dark brown. The characteristic absorption band of AgNPs was observed at 415 nm for *Echinops ritro* L(Fig.1) due to localized plasmon resonance (LSPR). This property appears on the surface of certain metals and results from the collective movement of free electrons in the nanoparticle when light falls on it [36]. Similar visual observation was found in AgNPs synthesized from *Prosopis juliflora* extract [37].

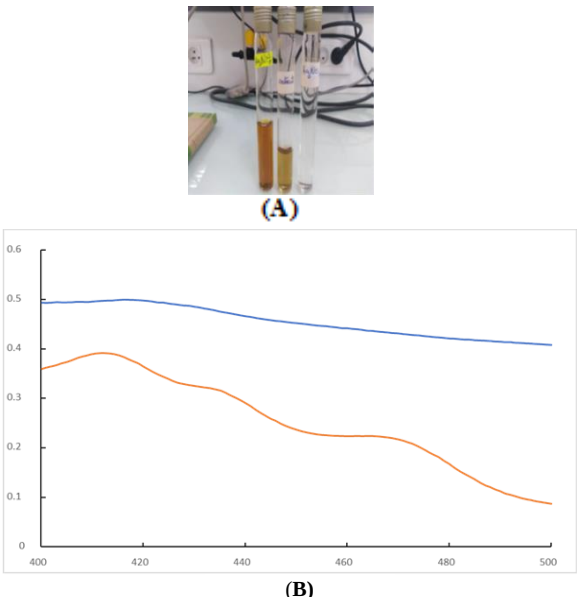

Figure .1 Colour change in the reaction mixture indicate formation of AgNPs (**A).** UV-Visible spectrum of AgNPs (**B).**

3.1.2. Fourier Transform Infra-Red Spectroscopy

The Fourier Transform Infrared (FTIR) technique was developed to detect potential biomolecules involved in silver ion reduction and bio-reduced silver nanoparticle capping.

The comparison between the FTIR spectrum of the *Echinops ritro* L ethanolic extract (Fig.2) and the curve of the silver nanoparticles (Fig.3) formed reveals variations in intensity at several peaks in various spectrum regions.

The AgNPs sample shows peaks (Fig.3) at 3300, 2999, 1651, 1400, 1053, 887 and 555 cm^{-1}. The band seen at 3300 cm^{-1} corresponds to the O−H functional groups found in phenols and flavonoids. The bands observed at 2999 cm^{-1} may be attributed to the existence of aliphatic C−H functional groups. The absorption peak corresponding to C=C stretching vibration appeared at 1651 cm^{-1}. The characteristic of a strong peak of the C−O band can be seen at 1053 cm^{-1}

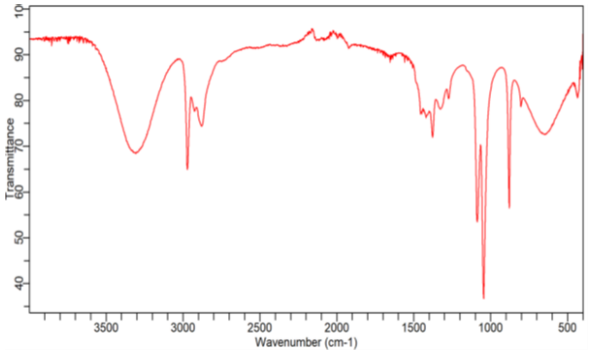

Figure 2. Fourier Transform Infra-red spectroscopy (FTIR) spectrum of the ethanolic extract.

The appearance of a broad characteristic band on the spectrum of nanoparticles observed at 555 cm^{-1} attributed to the formation of salts and probably in our spectrum indicates the formation of Ag NPs bonds [38]. The comparison of the two spectra (Fig.2) revealed that after encapsulation, the peaks are narrower and shifted, which indicates that the groups are converted to reduce Ag+ ions to Ag° present in ethanolic extract.

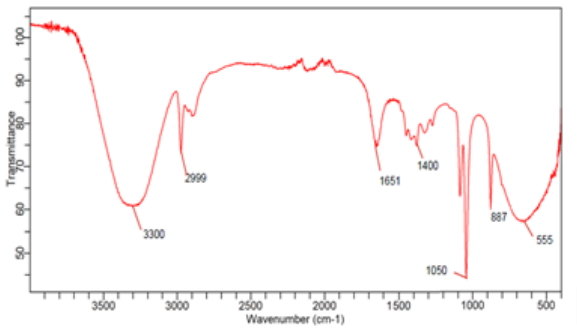

Figure3. Fourier Transform Infra-red spectroscopy (FTIR) spectrum of the biosynthesized AgNPs.

3.1.3.X-ray diffractometry

XRD performed a structural analysis of silver nanoparticles prepared from the sample (fig.4). They are considering the angular positions of the Bragg peaks. Seven prominent characteristic diffraction peaks for silver were observed at 27.7°, 32.2°,38°,46°,54.8°,57.5°,76.8° of 2θ values due to reflection from the crystal facet of (1 1 1) (2 0 0) (1 1 1) (2 2 0) (3 1 1) (2 2 2) (3 1 1) respectively, which may be indexed based on the face-centered cubic structure of AgNPs .XRD confirms the crystalline

nature of the nanoparticles. The comparison of the results on the nanometric scale indicates that the size of the silver nanoparticles formed in part of the extract of *Echinops ritro L* is 23.36 nm. The AgNPs synthesized from *Streblus asper* leaves exhibited similar diffraction peaks, suggesting they have a face-centered cubic (FCC) crystal structure [39].

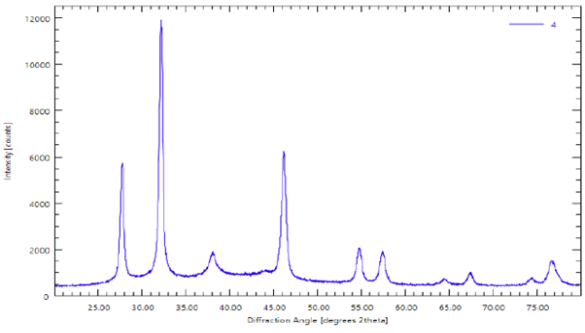

Figure 4. X-ray diffraction pattern of of AgNPs

3.2. Antimicrobial activity

Five microbial strains and one fungus strain were selected for antimicrobial activity of our compounds at different concentrations by measuring the diameter of inhibition zones or the absence thereof according to National Committee for Clinical Laboratories Standard rules [40], indicating either inhibition or lack of inhibition of bacterial growth. The presence of antibacterial activity is marked by clear zones appearing around the paper discs impregnated with different test products. The absence of inhibition is indicated by the lack of clear zones (halos) around the discs. The diameter of these inhibition zones varies depending on the bacterial strain being tested. In this study, the products are tested against five bacterial strains belonging to the American Type Culture Collection ATCC.

This approach allows for assessing the synthesized nanoparticles effectiveness in inhibiting the growth of specific bacterial strains, providing insights into their potential as antimicrobial agents. Our results revealed zones of inhibition greater than 5mm, varying across different strains (Table 1). The results obtained demonstrated that the biological efficacy of the AgNPs against all strains is directly proportional to the increase in concentrations, indicating that the concentration of the extract used had an influence on their susceptibility or resistance. Meaning that the higher the concentration, the more the AgNPs inhibits bacteria growth [41]. The highest antibacterial activity was observed against E. coli with inhibition zone of 33mm for 100µg/ml of AgNPs at followed by Enterococcus hirae with inhibition zone of 30 mm for 100µg/ml, Proteus species, Enterococcus faecalis, and Bacillus cereus, and least inhibition zone was observed against Staphylococcus aureus (5 mm) at 2.5 (µg/mL), (Fig.5; Fig.6).

This sensitivity may be related to structural variations in the cell walls of Gram-positive and Gram-negative bacteria [41].

Our findings contrast those of Fleurette et al. (1995) [42], who argue that Gram-positive bacteria are more resistant to antimicrobial agent due to the unique chemical composition of their cell walls. Gram-negative bacteria have a wall that allows lipophilic molecules to penetrate, and the presence of negatively charged lipopolysaccharides (LPS) promotes nanoparticle adherence. Gram-positive bacteria, on the other hand, are predominantly made up of peptidoglycans, which facilitate the passage of hydrophilic molecules [43.44].

However, according to all published work regarding the effectiveness of silver nanoparticles against the *Candida* fungus, it was weak compared to the biological effectiveness against bacteria, the value did not exceed 21mm at the highest concentration, which is estimated at100µg/mL. Studies suggest that silver ions' antimicrobial activity stems from their positive charge, which allows them to interact electrostatically with the negatively charged cell membranes of microorganisms [45]

The antimicrobial effectiveness of AgNPs may be linked to their size, enabling interaction with bacterial cells via transmembrane proteins. Upon binding, structural changes occur, blocking transport channels [46]. This process hinges on NP size, with smaller NPs (250 times smaller than bacteria) proving more efficient. They attach to wall proteins' (-SH) groups, penetrate membranes, alter permeability, and induce cell lysis [47–49]. Conversely, larger NPs with greater absolute surface area enhance adhesion via van der Waals forces, leading to internalization, ionization inside cells, structural damage, and ultimately, cell death [50]. In addition, the interaction of silver particles with thiol group molecules prevalent in bacterial respiratory enzymes is responsible for their antibacterial activity. Silver attaches to the bacterial cell wall and membrane, inhibiting the respiration process. AgNPs preferentially target the respiratory chain. [51].

Table 1. The average diameter of the silver nanoparticles' zone of inhibition (measured in millimetres) against bacterial and fungal species.

Bacterial species	Concentration of AgNPs (µg/mL)						
	2.5	5	10	50	100	Positive Control	Negative control (DMSO)
	Inhibition zones (mm)						
E. coli	09±0.57	17±3.51	20±5.00	24±6.00	33±12.5	35±0.00	0
Proteus mirabilis	06±0.00	11±3.60	16±2.00	18±1.52	27±6.50	33±0.00	0
Enterococcus faecalis	12±0.00	17±1.15	19±0.00	20±0.00	20±0.00	41±0.00	0
Enterococcus hirae	05±0.00	16±1.15	25±0.00	30±0.00	30±0.00	46±0.00	0
Bacillus cereus	6±0.00	11±0.00	16±0.00	17±0.0.	19±0.00	37±0.00	0
Fungal species	Inhibition zones (mm)						
Candida albicans	11±0.57	13±2.08	15±1.52	15±0.57	21±1.00	0	33±1.52

Values are expressed as Mean ± SE (n =3)

The generation of reactive oxygen species (ROS) by metal NPs is identified as a potential mechanism for their bactericidal action, damaging peptidoglycans, cell membranes, DNA, mRNA, ribosomes, and proteins [49]. ROS also hinders transcription, translation, and enzymatic functions and disrupts the electron transport chain, particularly in metal oxide NPs where ROS production is a primary toxicity mechanism [52, 53]. Metal oxide NPs can deactivate proteins and harm DNA by binding metal ions to enzyme thiol groups, disrupting hydrogen bonds between pyrimidine and purine base pairs and ultimately damaging the DNA molecule [54].

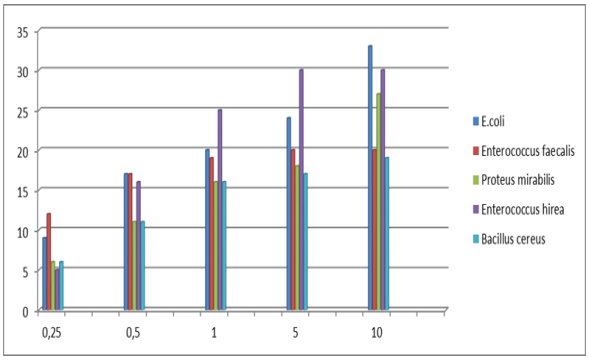

Figure 5. Inhibition zone of AgNPs of *Echinops ritro* L

4.Conclusion

Antimicrobial agents are increasingly becoming resistant to a wide range of antibiotics, creating an urgent need for alternative strategies to combat drug-resistant microorganisms. Silver ions and silver salts have long been used as antimicrobial agents across various fields due to their ability to inhibit microbial growth. However, their use comes with limitations, such as interference from salts, which can reduce their effectiveness. These challenges can be overcome by utilizing silver in nanoparticle form. The nano size increases the surface area, enhancing the interaction between Ag (0) and microorganisms. To apply AgNPs in diverse fields, it is essential to develop environmentally friendly synthesis methods, does not contain toxic components, and is suitable for pharmaceutical and biological applications [55].

In this study, we present a green, cost-effective approach to prepare AgNPs that is both eco-friendly and efficient using an ethanolic extract of the *Echinops ritro* L. These biosynthetized AgNPs were then used to demonstrate antimicrobial activity.

The results confirmed the crystalline nature of the silver nanoparticles synthesized by ethanolic extract from the aerial part of Echinopsritro L, with an average particle size of 23 nm, and were primarily spherical in shape.

A significant zone of inhibition for E. coli was achieved using AgNPs (33 mm) at a concentration of 100 µg/mL of silver nanoparticles. Nanoparticles at different concentrations showed antibacterial activity against all the strains of bacteria tested. The AgNPs exhibited antifungal properties against Candida albicans. The highest zone of inhibition diameter obtained was 17 mm when 100 µg/mL of the nanoparticles (AgNP3) was used. It was concluded that nanoparticles have bacteriostatic characteristics at low concentrations. Therefore, these nanoparticles are considered effective in preventing bacterial contamination.

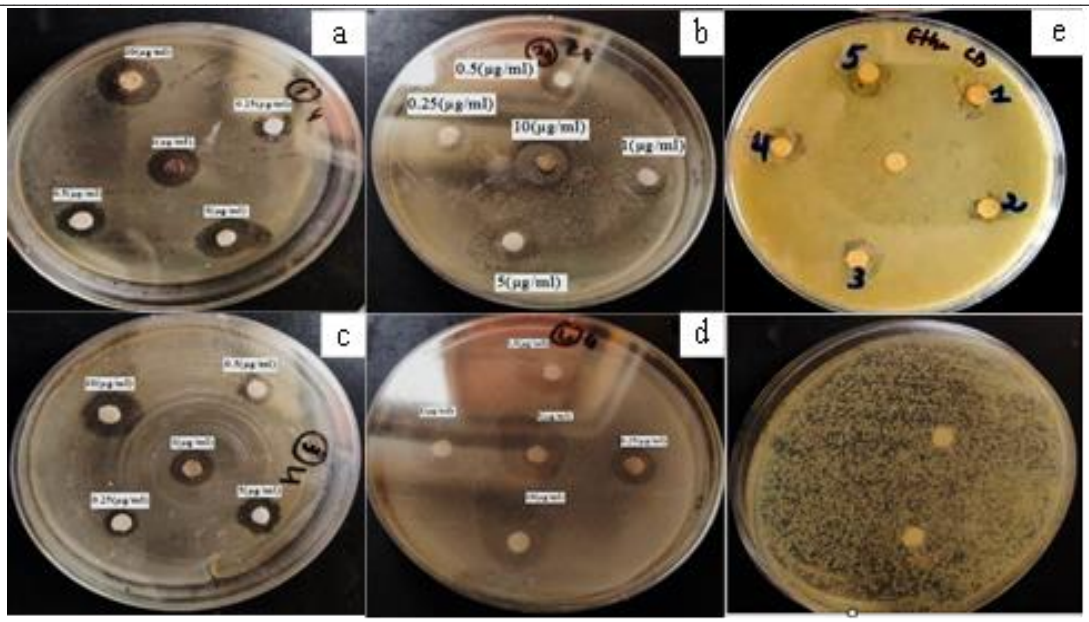

Figure 6. Antimicrobial activity of AgNPs synthesized by *Echinops ritro* L extract (a) *.E.Coli ,(b). Proteus mirabilis .(c). Enterococcus hirea.(d). Bacillus cereus.(e) Candida albicans. Control DMSO(f)*

5.Conflict of interest

There is no conflict of interest for any of the contributing authors.

6.Formatting of funding sources

No fund received to carry out this work.

7.Acknowledgment

The authors of this work would like to thank the staff of the scientific and technical research unit in physicochemical analysis of Biskra university for the provision of UV, FTIR and XRD facilities.

8.References

[1] Brives, C. (2024). Pluribiose: Travailler avec les microbes (p. 79). Éditions Quae.

[2] Sender, R., Fuchs, S., & Milo, R. (2016). Revised estimates for the number of human and bacteria cells in the body. PLoS biology, 14(8), e1002533.

[3] Dekaboruah, E., Suryavanshi, M. V., Chettri, D., & Verma, A. K. (2020). Human microbiome: an academic update on human body site specific surveillance and its possible role. Archives of microbiology, 202, 2147-2167.

[4] Robinson, C. M., & Pfeiffer, J. K. (2014). Viruses and the microbiota. Annual review of virology, 1(1), 55-69.

[5] Soni, J., Sinha, S., & Pandey, R. (2024). Understanding bacterial pathogenicity: a closer look at the journey of harmful microbes. Frontiers in Microbiology, 15, 1370818.

[6] Ikuta, K. S., Swetschinski, L. R., Aguilar, G. R., Sharara, F., Mestrovic, T., Gray, A. P., ... & Dhingra, S. (2022). Global mortality associated with 33 bacterial pathogens in 2019: a systematic analysis for the Global Burden of Disease Study 2019. The Lancet, 400(10369), 2221-2248.

[7] Dadi, R. (2019). Synthèse de nanoparticules d ‘oxydes métalliques et leur activité antibactérienne (Doctoral dissertation, Université Paris-Nord-Paris XIII).

[8] Baek Y.-W., An Y.-J. Microbial toxicity of metal oxide nanoparticles (CuO, NiO, ZnO, and Sb2O3) to Escherichia coli, Bacillus subtilis, and Staphylococcus aureus. The Science of the Total Environment. 2011;409(8):1603–1608

[9] A.-P. Magiorakos, A. Srinivasan, R. B. Carey et al., « Multidrug-resistant, extensively drug-resistant and pandrug-resistant bacteria: an international expert proposal for interim standard definitions for acquired resistance, » Clinical Microbiology and Infection, vol. 18, no. 3, pp. 268–281, 2012.

[10] Horan TC, Gaynes RP. Surveillance of nosocomial infections. In: Mayhall CG, editor. « Hospital epidemiology and infection control », Philadelphia: Lippincott Williams and Wilkins; . pp. 1659–702, 2004.

[11] Grohskopf LA, Sinkowitz-Cochran RL, Garrett DO, Sohn AH, Levine GL, Siegel JD, et al. « A national point-prevalence survey of paediatric intensive care unit-acquired infections in the United States », J Pediatr. 140:432–8, 2002.

[12] Rosi NL, Mirkin CA. Nanostructures in bio diagnostics. Chem Rev. 2005; 105:1547-1562. [10] Raghupati KR, KOOdali RT, Manna AC. Size-dependent bacterial growth inhibition and mechanism of antibacterial activity of zinc

oxide nanoparticles. Langmuir. 2011; 27: 4020-4028.
[13] Lewis K, Klibanov AM. Surpassing nature: rational design of sterile-surface materials. Trends Biotechnol. 2005; 23:343-348. 147
[14] Azam A, Ahmed AS, Oves M, Khan MS, Memic A. Size-dependent antimicrobial properties of CuO nanoparticles against Gram-positive and –negative bacterial strains. Int J Nanomédecine. 2012; 7:3527-3535.
[15] Zeyons, O. (2008). Etudes des interactions physicochimiques et biologiques entre des nanoparticules manufacturées et des bactéries de l'environnement (Doctoral dissertation, Université Pierre et Marie Curie-Paris VI).
[16] Jung,W.K.; Koo, H.C.; Kim, K.W.; Shin, S.; Kim, S.H.; Park, Y.H. Antibacterial activity and mechanism of action of the silver ion in staphylococcus aureus and escherichia coli. Appl. Environ. Microbiol. 2008, 74,2171–2178.
[17] Morones-Ramirez, J.R.; Winkler, J.A.; Spina, C.S.; Collins, J.J. Silver enhances antibiotic activity against gram-negative bacteria. Sci. Transl. Med. 2013, 5, 190ra181
[18] Yakabe, Y.; Sano, T.; Ushio, H.; Yasunaga, T. Kinetic studies of the interaction between silver ion and deoxyribonucleic acid. Chem. Lett. 1980, 9, 373–376
[19] Mikhailova, E. O. (2020). Silver nanoparticles: Mechanism of action and probable bio-application. Journal of functional biomaterials, 11(4), 84.
[20] Huang J., Lin L., Sun D., Chen H., Yang D., Li Q. Bio-inspired synthesis of metal nanomaterials and applications. Chem. Soc. Rev. 2015; 44:6330–6374
[21] Singh P., Pandit S., Beshay M., Mokkapati V.R.S.S., Garnaes J., Olsson M.E., Sultan A., Mackevica A., Mateiu R.V., Lütken H., et al. Anti-biofilm effects of gold and silver nanoparticles synthesized by the Rhodiola rosea rhizome extracts. Artif. Cells Nanomed. Biotechnol. 2018; 46:886–899.
[22] Kasithevar M., Saravanan M., Prakash P., Kumar H., Ovais M., Barabadi H., Shinwari Z.K. Green synthesis of silver nanoparticles using Alysicarpusmonilifer leaf extract and its antibacterial activity against MRSA and CoNS isolates in HIV patients. J. Interdiscip. Nanomed. 2017; 2:131–141.
[23] Benakashani F., Allafchian A.R., Jalali S.A.H. Biosynthesis of silver nanoparticles using Capparis spinosa L. leaf extract and their antibacterial activity. Karbala Int. J. Mod. Sci. 2016; 2:251–258
[24] Mandal P., Babu S.S., Mandal N. Antimicrobial activity of saponins from Acacia auriculiformis. Fitoterapia. 2005; 76:462–465.
[25] Ahmad N., Sharma S. Green synthesis of silver nanoparticles using extracts of Ananas comosus. Green Sustain. Chem. 2012; 2:141–147.
[26]. Marimuthu S., Rahuman A.A., Rajakumar G., Santhoshkumar T., Kirthi A.V., Jayaseelan C., Bagavan A., Zahir A.A., Elango G., Kamaraj C. Evaluation of green synthesized silver nanoparticles against parasites. Parasitol. Res. 2011; 108:1541–1549.
[27] Elavazhagan T., Arunachalam K.D. Memecylonedule leaf extract mediated green synthesis of silver and gold nanoparticles. Int. J. Nanomed. 2011; 6:1265–1278.
[28] Bhadra M.P., Sreedhar B., Patra C.R. Potential theranostics application of bio-synthesized silver nanoparticles (4-in-1 system) Theranostics. 2014; 4:316–335.
[29] Patra S., Mukherjee S., Barui A.K., Ganguly A., Sreedhar B., Patra C.R. Green synthesis, characterization of gold and silver nanoparticles and their potential application for cancer therapeutics. Mater. Sci. Eng. C. 2015; 53:298–309.
[30] Khan M.A., Khan T., Nadhman A. Applications of plant terpenoids in the synthesis of colloidal silver nanoparticles. Adv. Colloid Interface Sci. 2016; 234:132–141
[31] Aydın, Ç., Özcan, G. T., Turan, M., & Mammadov, R. (2016). Phenolic contents and antioxidant properties of *Echinops ritro* L. and E. tournefortiiJaup. Et. Spachextract. International Journal of Secondary Metabolite, 3(2), 74-81.
[32] Laouedj M. (2016), Posologies des plantes médicinales d'Algérie Deuxième partie. l‟édition ed ilivre Paris.p188 .
[33]. Zafar, S., Faisal, S., Jan, H.,Ullah, R., Rizwan, M., Abdullah , &Khattak, A. (2022). Development of iron nanoparticles (FeNPs)using biomass of enterobacter: its characterization, antimicrobial, anti-Alzheimer's, and enzyme inhibition potential. Micromachines,13(8), 1259. doi: 10.3390/mi13081259
[34] Abomuti MA, Danish EY, FirozA, et al. Green synthesis of zincoxide nanoparticles using salvia officinalis leaf extract and theirphotocatalytic and antifungal activities. Biology. 2021;10(11): 1075.doi: 10.3390/biology1011107.
[35] johnson P, Krishnan V, Loganathan C, et al. Rapid biosynthesis of Bauhinia variegata flower extract-mediated silver nanoparticles: an

effective antioxidant scavenger and a-amylase inhibitor. Artif Cells Nanomed Biotechnol. 2018;46(7):1488–1494.

[36] Jussila, H., Yang, H., Granqvist, N., & Sun, Z. (2016). Surface plasmon resonance for characterization of large-area atomic-layer graphene film. Optica, 3(2), 151-158.

[37].Arya G, Kumari RM, Gupta N, et al. Green synthesis of silver nanoparticles using Prosopis juliflora bark extract: reaction optimization, antimicrobial and catalytic activities. Artif Cells Nanomed Biotechnol. 2018;46(5):985–993

[38] Geetha, R., Ashokkumar, T., Tamilselvan, S., Govindaraju, K., Sadiq, M., &Singaravelu, G. (2013). Green synthesis of gold nanoparticles and their anticancer activity. Cancer Nanotechnology, 4, 91-98.

[39]. Das S, Das A, Maji A, et al. A compact study on impact of multiplicative *Streblus asper* inspired biogenic silver nanoparticles as effective photocatalyst, good antibacterial agent and interplay upon interaction with human serum albumin. J Mol Liq. 2018; 259:18–29

[40] PA, W. (2010). Clinical and Laboratory Standards Institute: Performance standards for antimicrobial susceptibility testing: 20th informational supplement. CLSI document M100-S20.

[41] Roy, S., &Rhim, J. W. (2019). Carrageenan-based antimicrobial bionanocomposite films incorporated with ZnO nanoparticles stabilized by melanin. Food Hydrocolloids, 90, 500-507.

[42] J.J. Fleurette, M. Freney, E. Reverdy. (1995). Antiseptie etdésinfection. Paris: ESKA Editions.

[43] M.S. Ali-Shtayeh, R.M.-R. Yaghmour, Y.R. Faidi, et al. Antimicrobial activity of 20 plants used in folkloric medicine in the Palestinian area. Journal of Ethno Pharmacology, 1998, 60: 265−271. https://doi.org/10. 1016/s0378-8741(97)00153-0

[44] Haddi, R., El Kharraz, A. M., & Kerroumi, M. I. (2024). Green Synthesis of Zinc Oxide Nanoparticles Using Pistacia lentiscus L. Leaf Extact and Evaluating their Antioxydant and Antibacterial Properties. *Nano Biomedicine & Engineering*, *16*(2).

[45] Dibrov, P., Dzioba, J., Gosink, K. K., & Häse, C. C. (2002). Chemiosmotic mechanism of antimicrobial activity of Ag+ in Vibrio cholerae. *Antimicrobial agents and chemotherapy*, *46*(8), 2668-2670.

[46] Zhang, H., & Chen, G. (2009). Potent antibacterial activities of Ag/TiO2 nanocomposite powders synthesized by a one-pot sol− gel method. Environmental science & technology, 43(8), 2905-2910.

[47] Kairyte, K., Kadys, A., &Luksiene, Z. (2013). Antibacterial and antifungal activity of photoactivated ZnO nanoparticles in suspension. Journal of Photochemistry and Photobiology B: Biology, 128, 78-84.

[48] Sirelkhatim, A., Mahmud, S., Seeni, A., Kaus, N. H. M., Ann, L. C., Bakhori, S. K. M., ... & Mohamad, D. (2015). Review on zinc oxide nanoparticles: antibacterial activity and toxicity mechanism. Nano-micro letters, 7, 219-242.

[49] Huang, Y. W., Wu, C. H., &Aronstam, R. S. (2010). Toxicity of transition metal oxide nanoparticles: recent insights from in vitro studies. Materials, 3(10), 4842-4859.

[50] Huang, Z., Zheng, X., Yan, D., Yin, G., Liao, X., Kang, Y., ... & Hao, B. (2008). Toxicological effect of ZnO nanoparticles based on bacteria. Langmuir, 24(8), 4140-4144.

[51] M. Rai, A. Yadav, A. Gade, Silver nanoparticles as a new generation of antimicrobials, Biotechnol. Adv. 27 (2009) 76–83.

[52] Hajipour, M. J., Fromm, K. M., Ashkarran, A. A., de Aberasturi, D. J., de Larramendi, I. R., Rojo, T., ... &Mahmoudi, M. (2012). Antibacterial properties of nanoparticles. Trends in biotechnology, 30(10), 499-511.

[53] Kumar, A., Pandey, A. K., Singh, S. S., Shanker, R., & Dhawan, A. (2011). Engineered ZnO and TiO2 nanoparticles induce oxidative stress and DNA damage leading to reduced viability of Escherichia coli. Free Radical Biology and Medicine, 51(10), 1872-1881.

[54] Xia, Z., Min, J., Zhou, S., Ma, H., Zhang, B., & Tang, X. (2021). Photocatalytic performance and antibacterial mechanism of Cu/Ag-molybdate powder material. Ceramics International, 47(9), 12667-12679.

[55] Silver S, Phung LT: Bacterial heavy metal resistance: new surprises. Annu Rev Microbiol 1996, 50: 753-789.10.1146/annurev.micro.50.1.753